NeuroImage 55 (2011) 1528–1535

Contents lists available at ScienceDirect

NeuroImage

journal homepage: www.elsevier.com/locate/ynimg

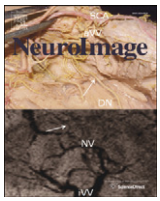

A novel method for reliable and fast extraction of neuronal EEG/MEG oscillations on the basis of spatio-spectral decomposition

Vadim V. Nikulin [a,b,*], Guido Nolte [c], Gabriel Curio [a,b]

[a] Neurophysics Group, Department of Neurology, Campus Benjamin Franklin, Charité - University Medicine Berlin, D-12200 Berlin, Germany
[b] Bernstein Center for Computational Neuroscience, Berlin, Germany
[c] Fraunhofer FIRST, D-12489 Berlin, Germany

ARTICLE INFO

Article history:
Received 6 October 2010
Revised 13 December 2010
Accepted 20 January 2011
Available online 27 January 2011

Keywords:
Oscillations
Synchronization
EEG
MEG
Alpha

ABSTRACT

Neuronal oscillations have been shown to underlie various cognitive, perceptual and motor functions in the brain. However, studying these oscillations is notoriously difficult with EEG/MEG recordings due to a massive overlap of activity from multiple sources and also due to the strong background noise. Here we present a novel method for the reliable and fast extraction of neuronal oscillations from multi-channel EEG/MEG/LFP recordings. The method is based on a linear decomposition of recordings: it maximizes the signal power at a peak frequency while simultaneously minimizing it at the neighboring, surrounding frequency bins. Such procedure leads to the optimization of signal-to-noise ratio and allows extraction of components with a characteristic "peaky" spectral profile, which is typical for oscillatory processes. We refer to this method as spatio-spectral decomposition (SSD). Our simulations demonstrate that the method allows extraction of oscillatory signals even with a signal-to-noise ratio as low as 1:10. The SSD also outperformed conventional approaches based on independent component analysis. Using real EEG data we also show that SSD allows extraction of neuronal oscillations (e.g., in alpha frequency range) with high signal-to-noise ratio and with the spatial patterns corresponding to central and occipito-parietal sources. Importantly, running time for SSD is only a few milliseconds, which clearly distinguishes it from other extraction techniques usually requiring minutes or even hours of computational time. Due to the high accuracy and speed, we suggest that SSD can be used as a reliable method for the extraction of neuronal oscillations from multi-channel electrophysiological recordings.

Introduction

Neuronal oscillations constitute a major operational mode of brain activity. Many studies have shown that they underlie perceptual, cognitive and motor functions (for reviews see: Buzsáki and Draguhn, 2004; Varela et al., 2001). Neuronal oscillations are ubiquitous, they are generated in almost any area of the cortex as well as in the subcortical structures, such as basal ganglia and thalamus (Steriade, 2001). Yet, exactly because there are so many sources of neuronal oscillations, as well as a massive amount of background neuronal noise, it is difficult to extract distinct sources of oscillatory activity. This holds not only for non-invasive electrophysiological measures, such as EEG/MEG, but also for the invasive approaches, such as electro-corticographic recordings in patients.

Different decomposition techniques have been proposed for extracting neuronal oscillations. In EEG/MEG research frequently used algorithms are based on independent component analysis (ICA) not requiring inverse modeling calculations. ICA extracts independent sources by exploiting non-Gaussianity of the sources (Hyvärinen et al., 2001), e.g., through the maximization of kurtosis, hyperbolic tangent, skewness (FastICA algorithm, Hyvärinen and Oja, 1997) or maximizing information (infomax approach, Bell and Sejnowski, 1995). Another class of ICA approaches utilizes temporal structure/spectral differences between the sources (SOBI approach, Belouchrani et al., 1997; Tang et al., 2005; or TDSEP/ffdiag approach, Ziehe et al., 2004). Importantly, as noted by Hyvärinen et al. (2010) similar spectra indicate similar (statistically) temporal correlations and vice versa due to Wiener–Khinchin theorem. Moreover, Ziehe et al. (2000) showed that decorrelation in time domain is equivalent to exploiting different spectral content of the sources in the Fourier domain. These ICA approaches might meet intrinsic limitations for regular EEG/MEG oscillatory components which not only represent a mixture of relatively narrow-band signals with very similar spectra but are also fairly Gaussian distributed due to the amplitude modulation of oscillatory sources (Hyvärinen et al., 2010). Moreover, the majority

Abbreviations: CSP, common spatial patterns; ICA, independent component analysis; SOBI, second-order blind identification algorithm; SSD, spatio-spectral decomposition; SNR, signal-to-noise ratio.

* Corresponding author at: Department of Neurology, Charité - University Medicine Berlin, D-12200 Berlin, Germany. Fax: +49 30 8445 4264.
E-mail address: vadim.nikulin@charite.de (V.V. Nikulin).

1053-8119/$ – see front matter © 2011 Elsevier Inc. All rights reserved.
doi:10.1016/j.neuroimage.2011.01.057

of ICA methods are based on numerical approaches, which do not always guarantee adequately converging solutions, and in addition, computing ICA can be time consuming.

Here we introduce a novel method for the separation of oscillatory sources from a set of mixed signals, which is a common problem in EEG/MEG research. This method is based on a linear decomposition of the recorded EEG/MEG signals guided by the objective to maximize power at a peak frequency of oscillations and simultaneously minimize the power at the neighboring frequency bins. We show that such decomposition is equivalent to the maximization of signal-to-noise ratio (SNR) and that it produces components with spectral profiles characteristic for oscillatory sources. We refer to this method as spatio-spectral decomposition (SSD). We present below a theoretical basis for its efficiency to extract oscillatory activity, validate the method with simulations, and present a first exemplary analysis of real EEG data.

Material and methods

Motivation

Often signal and noise have overlapping frequency content and thus their separation becomes difficult. A frequently used approach is to record EEG/MEG activity in two different time windows corresponding to a predominant presence of either noise or signal of interest (Koles, 1991). However, there is not always a possibility to record different sessions with either noise or signal. Therefore from both the algorithmical and practical point of view it would be desirable to estimate noise and signal parameters from the same measurement.

An important assumption of our approach is that noise sources produce signals with a relatively broad frequency range, e.g., from few Hz to tens of Hz. In many cases the noise sources are modeled either as white or *1/f* noise, the latter being typical for many experimentally obtained LFP and EEG/MEG recordings. Because the noise is spectrally extended we can use frequency bins around the frequency range of interest in order to enhance the SNR by estimating the noise in the spectral neighborhood of the frequency range of interest. Algorithmically, one minimizes the variance of the noise around the spectral peak of interest while simultaneously maximizing the variance of the signal at the peak frequency (Fig. 1). In the Fourier domain this leads to a typical "peaky" profile of the spectrum with large power P at a central peak flanked by considerably smaller power at the neighboring frequency bins, i.e., $P(f-\Delta f)<P(f)$ and $P(f)>P(f+\Delta f)$, representing the characteristic shape of a spectrum for signals with good SNR. Such simultaneous minimization of surrounding noise and maximization of the signal at the peak frequency can be achieved straightforwardly with diagonalization of two covariance matrices corresponding to the signal of interest and the surrounding "flanking" noise. Below we elaborate on the details of our approach.

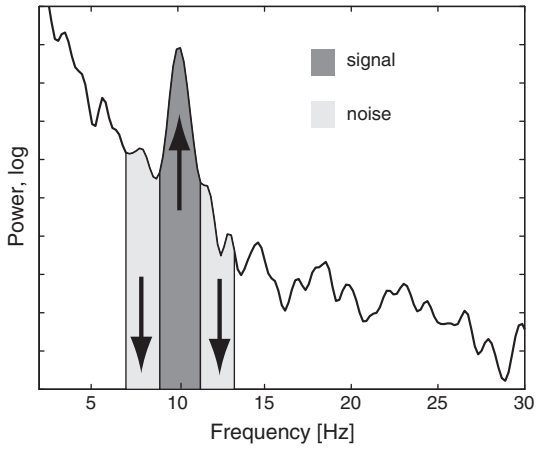

Fig. 1. A schematic explanation of spatio-spectral decomposition algorithm. The main idea of SSD is to find linear filters which maximize the power in the frequency band of studied neuronal oscillations while minimizing the power at the neighboring "flanking" frequency bins. Such procedure results in the extraction of the components, which have characteristic "peaky" spectrum typical for oscillatory signals.

Spectral ratios

We assume an additive model for the signal s and noise n such that the measured activity m is expressed as:

$$m = s + n \tag{1}$$

SNR in one sensor for frequency f is defined as:

$$SNR = \frac{P_s(f)}{P_n(f)} \tag{2}$$

where P_s and P_n are the powers at the frequency f for the signal and noise, respectively.

In general, we are interested in extracting oscillatory activity and thus the spectrum of s is restricted to a small frequency range. In addition we also assume that the noise spectrum is relatively monotonous/smooth and in general its power is proportional to $1/f^{\alpha}$ (for up to tens of Hz), where $\alpha=0$ and $\alpha=1$ correspond to white and *1/f* types of noise, respectively, the latter being the most common noise encountered in EEG and MEG recordings.

Usually SNR cannot be reliably assessed from the recordings due to the overlap of s and n at the frequency f. Instead, we show below that one can express SNR using different frequency bins, i.e., $f-\Delta f$ and $f+\Delta f$.

If frequencies $f-\Delta f$ and $f+\Delta f$ are outside of the spectral peak of s and Δf is relatively small then:

$$P_n(f)\approx[P_m(f-\Delta f)+P_m(f+\Delta f)]/2. \tag{3}$$

This is a linear approximation of the noise spectrum in the frequency neighborhood of f.

Recall that:

$$\left\langle |F_m(f)|^2 \right\rangle = \left\langle |F_s(f)|^2 \right\rangle + \left\langle |F_n(f)|^2 \right\rangle + 2\Re\langle F_s(f)F_n^*(f)\rangle \tag{4}$$

where $F_m(f)$, $F_s(f)$ and $F_n(f)$ are the Fourier transforms of the signals m, s and n, respectively.

If s and n are uncorrelated then $\Re\langle F_s(f)F_n^*(f)\rangle=0$ and thus Eq. (4) is reduced to:

$$\left\langle |F_m(f)|^2 \right\rangle = \left\langle |F_s(f)|^2 \right\rangle + \left\langle |F_n(f)|^2 \right\rangle \tag{5}$$

or

$$P_m(f) = P_s(f) + P_n(f). \tag{6}$$

Taking into account Eqs. (3) and (6) we can write:

$$\frac{P_m(f)}{[P_m(f-\Delta f)+P_m(f+\Delta f)]} \approx \frac{P_s(f)+P_n(f)}{2P_n(f)} = 0.5\left(\frac{P_s(f)}{P_n(f)}+1\right). \tag{7}$$

This indicates that the increase of the ratio in the left part of Eq. (7) should also lead to the increase in SNR defined in Eq. (2).

Algorithm

Taking into account the considerations provided above, we show how to find spatial filters which would maximize SNR for the EEG/

MEG recordings. We start with $t \times k$ measurement matrix M, where t is the number of samples and k is the number of channels. Assuming additivity of noise and signal the matrix can be written as:

$$M = S + N \tag{8}$$

where S and N correspond to signal and noise components, respectively.

We then proceed with the filtering of each column in M in two different ways. 1) M is filtered around signal frequency f and leads to the matrix M_s. 2) Next we filter M separately around the frequencies $f-\Delta f$ and $f+\Delta f$ and sum the filtered signals, yielding the matrix M_n. Alternatively, M_n can be obtained by filtering M in the frequency range $[f-\Delta f{:}f+\Delta f]$ with the following subtraction of M_s. In addition M_n can also be obtained by filtering M in the frequency range $[f-\Delta f{:}f+\Delta f]$ and then performing band-stop filtering around frequency f. In principle Δf should be small, in order to get a better linear estimation of SNR. However, due to the spectral leakage caused by band-pass filtering, realistic values for Δf can be within 1–2 Hz.

Matrices M_s and M_n are of the same dimensions as M, and correspond to the frequency ranges of: 1) signal plus noise and 2) noise alone, respectively. The columns in each matrix are also centered to have a zero mean. Next, we estimate the time-averaged covariance matrices for M_s and M_n, respectively:

$$C_s = \frac{M_s^T M_s}{t} \tag{9}$$

$$C_n = \frac{M_n^T M_n}{t} \tag{10}$$

Now one should find spatial filters which would be related to high spectral peak (variance) at the frequency of interest and low variance of the noise in the surrounding frequency bins. Denoting such spatial filter as $\vec{w}$ the problem is hence to maximize:

$$SNR\left(\vec{w}\right) = \frac{\vec{w}^T C_s \vec{w}}{\vec{w}^T C_n \vec{w}} \tag{11}$$

which is a standard problem and leads to the generalized eigenvalue decomposition (Fukunaga, 1990):

$$C_s \vec{w} = \lambda C_n \vec{w}. \tag{12}$$

For the later discussion we reformulate the problem using a coordinate transformation. Defining 'whitened' filters and signal covariance as:

$$\vec{v} \equiv C_n^{1/2} \vec{w} \tag{13}$$

$$D_s \equiv C_n^{-1/2} C_s C_n^{-1/2}. \tag{14}$$

Then, Eq. (11) reads:

$$SNR\left(\vec{v}\right) = \frac{\vec{v}^T D_s \vec{v}}{\vec{v}^T \vec{v}} \tag{15}$$

and its maximization leads to the eigenvalue equation:

$$D_s \vec{v} = \lambda \vec{v}. \tag{16}$$

With k solutions $\vec{v}_i$ and λ_i for $i=1\ldots k$. Since D_s is a hermitian matrix, all eigenvectors are orthogonal, i.e. $\vec{v}_i^T \vec{v}_j = \delta_{ij}$, where δ_{ij} is a Kronecker's delta or, equivalently, for $V = \left(\vec{v}_1, \cdots, \vec{v}_k\right)$ we have:

$$V^{-1} = V^T. \tag{17}$$

If we now assume that the signal is generated from k uncorrelated sources the signal covariance matrix C_s has the form:

$$C_s = \sum_{i=1}^{k} \alpha_i \vec{a}_i \vec{a}_i^T \tag{18}$$

where $\vec{a}_i$ is the topography and α_i the variance of the *i-th* source. In the whitened space this covariance has the form

$$D_s = \sum_{i=1}^{k} \alpha_i \vec{b}_i \vec{b}_i^T \tag{19}$$

with $\vec{b}_i = C_n^{-1/2} \vec{a}_i$ which is identical to the eigenvalue decomposition provided that the $\vec{b}_i$ are orthogonal. In this case $\vec{b}_i$ is i-th eigenvector of D_s, i.e. $\vec{b}_i = \vec{v}_i$ and hence $\vec{v}_i = C_n^{-1/2} \vec{a}_i$. We emphasize here that the abovementioned holds only if $\vec{b}_i$ are orthogonal. Whether one can assume such orthogonality depends on the case considered. With realistic and hence correlated noise the whitening corresponds to a spatial high pass and dipolar patterns are mostly orthogonal in the whitened space (this also relates to source PCA and Minimum Overlap Component Analysis (Marzetti et al., 2008, please see Appendix A).

We finally go back to the original space to derive some relations between the spatial filter $\vec{w}_i$ and the corresponding topography $\vec{a}_i$, the former being one of the generalized eigenvectors of Eq. (12). Since $\vec{v}_i = C_n^{1/2} \vec{w}_i$ and $\vec{v}_i = C_n^{-1/2} \vec{a}_i$, for the latter assuming orthogonality of the topographies in the whitened space as discussed above, it follows that

$$\vec{a}_i = C_n \vec{w}_i \tag{20}$$

If we define $W = \left(\vec{w}_1, \cdots, \vec{w}_k\right)$ and $A = \left(\vec{a}_1, \cdots, \vec{a}_k\right)$ we can express this as

$$A = C_n W. \tag{21}$$

Recalling that $V = C_n^{1/2} W$ is orthogonal we get:

$$W^{-1} = \left(C_n^{-1/2} V\right)^{-1} = V^T C_n^{1/2} = (C_n W)^T = A^T. \tag{22}$$

In other words, the topographies can be calculated either by the inversion of W or by applying the noise covariance on it, and are contained in the respective rows.

Simulations

We simulated EEG recordings for 64 channels, which were fitted to the outermost layer of the standard Montreal Neurological Institute head (Evans et al., 1994). The head model was based on a three compartment realistic volume conductor and was used for calculation of EEG forward solutions (Nolte and Dassios, 2005). The sources were modeled as multiple current dipoles located in the triangularly tessellated cortical mantle. For the generation of noise we used 500 uncorrelated dipoles producing *1/f* type of noise. The dipoles had random spatial location and orientation. Importantly, this type of noise produces spatial correlations in the sensor space. The signal of interest was band-pass filtered white noise (10–12 Hz, frequency range as for the alpha oscillations). The simulations were performed for 5 alpha dipoles with random placement in the cortical grid and

random orientation. The duration of the simulated data was 125 s and sampling frequency 200 Hz. For simulations we used the following SNRs: 5, 1, 0.5, 0.25, 0.01, 0.05, and 0.01. For each SNR we performed 100 simulations with 5 dipoles. The SNR was calculated as the ratio between the mean variance across channels for each projected alpha dipole and the mean variance of additive *1/f* noise (produced by all noise dipoles) in the 10–12 Hz frequency range. In order to obtain the matrix M_s the data were filtered in the frequency range 10–12 Hz (we elaborate in the Discussion on the basic principles related to defining frequency bands when analyzing neuronal data). Matrix M_n was obtained by band-pass filtering data in the range 8–14 Hz and then performing in addition a band-stop filtering in the range 9–13 Hz (the cut-off frequencies for such band-stop filtering were selected to avoid spectral leakage from the signal part in 10–12 Hz range). Usually the filters do not have a box-car shape and there is a certain roll-off indicating that frequencies close to the edges of the filter contain non-zero power. Because of this there might be some residual oscillations present from the band-pass range in the flanking frequency bins and vice versa. Therefore filters should be designed to be sufficiently steep in order to prevent power leakage. In the present study we used band-stop filtering extending ± 1 Hz with respect to the band-pass filter edges. If the flanking frequency bins would contain part of the signal then SSD would not produce spatial filters optimal for the extraction of oscillatory sources, since the flanking covariance matrix M_n should ideally include only noise component. For a comparison we also utilized a second-order blind identification algorithm (SOBI, Belouchrani et al., 1997), which is one variant of ICA decomposition often used for the analysis of EEG/MEG signals. The main idea of SOBI is to minimize cross-correlations between the components at different time-lags. Algorithmically the method is based on simultaneous (approximate) diagonalization of many covariance matrices each corresponding to a specific delay. Such diagonalization procedure leads to temporally decorrelated components. For this algorithm we also performed a band-pass filtering in the 8–14 Hz frequency range and used 50 time-delayed covariance matrices with time delays of 5, 15, 25...495 ms. Thus, both SSD and SOBI algorithms used the same information in the relatively broad frequency range 8–14 Hz. However, further transformations with the data were performed differently for each algorithm. While SSD was based on forming two complementarily filtered data sets, SOBI proceeded with creating multiple time-delayed covariance matrices. We tested FastICA (Hyvärinen and Oja, 1997), with kurtosis or hyperbolic tangent as contrast functions, and found that it often did not converge and we dropped this algorithm from the present comparison. In addition we also tried to use ICA on the basis of the infomax approach (Bell and Sejnowski, 1995; Delorme and Makeig, 2004, authors' default settings). However, as in case of FastICA, infomax did not provide a satisfactory convergence of the solutions. Such performance of FastICA and infomax is most likely due to the very similar amplitude distributions of the band-pass filtered components.

The error between recovered and original pattern was calculated according to:

$$Err = 1 - \frac{\left| a_{or}^T a_r \right|}{||a_{or}|| \cdot ||a_r||} \tag{23}$$

where a_{or} are original patterns and a_r are patterns recovered through the SSD or ICA. Since there is no exact ordering of the recovered patterns we performed a pair-wise greedy search by first taking the pair with the smallest error, excluding this pair and continuing the pair matching. For both SSD and ICA we selected ten components with the largest spectral ratio, *R*:

$$R = \frac{P_f}{P_{sf}} \tag{24}$$

where P_f is a mean spectral power in the 10–12 Hz frequency range and P_{sf} is the combined mean spectral power in the 8–10 and 12–14 Hz frequency ranges (similar to the idea presented in Fig. 1).

Real EEG recordings

Seven subjects participated in the study (2 females). EEG recordings were performed at rest with subjects seated comfortably in the chair with their eyes open. The subjects were instructed to relax and to fixate their eyes on a mark in front of them. EEG data were recorded with 96 Ag/AgCl electrodes, using *BrainAmp* amplifiers and *BrainVision Recorder* software (Brain Products GmbH, Munich, Germany). The signals were

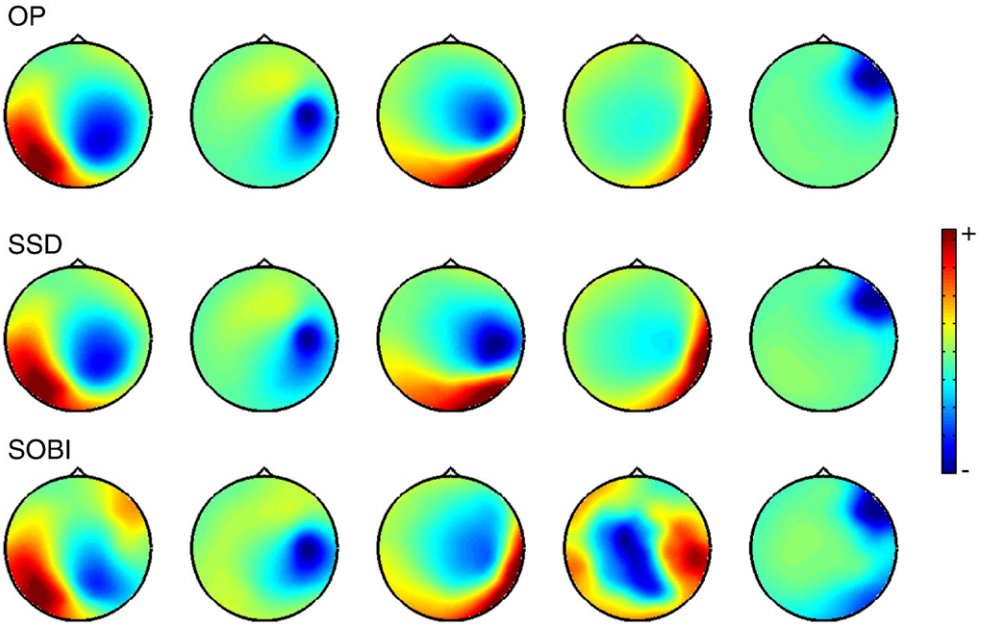

Fig. 2. An example of recovering patterns for simulated dipoles (SNR = 1). The upper row shows original patterns. The middle and lower rows—patterns obtained with SSD and SOBI algorithms, respectively. A global sign of patterns in SSD or SOBI was flipped in some cases in order to facilitate the comparisons with the original patterns. The color-scale is in arbitrary units.

recorded in a 0.1–250 Hz frequency range and digitized at 1000 Hz. For the following offline analysis the EEG data were decimated to 200 Hz.

In order to obtain the matrix M_s the data were filtered in the frequency range 8–13 Hz, matrix M_n was obtained by band-pass filtering data in the range 6–15 Hz and then performing in addition band-stop filtering in the range 7–14 Hz. The band-stop filter was designed to exclude the 8–13 Hz part of the EEG signal. For the SOBI algorithm we performed a band-pass filtering in the 6–15 Hz frequency range and used 50 time-delayed covariance matrices with time delays of 5, 15, 25...495 ms. Initial filtering in the 6–15 Hz frequency range ensured that both algorithms used as a starting point the same amount of information.

Results

Simulations

We performed simulations with different SNRs and calculated errors indicating how strongly the recovered topographies deviated from the simulated patterns.

Fig. 2 (top row) shows the original patterns for five exemplary dipoles with random locations and orientations while the second and third rows contain solutions provided by SSD and SOBI, respectively. The figure shows that SSD was capable of recovering sources with substantially overlapped topographies. The quantitative estimation of error across multiple simulations and for different SNRs is presented in Fig. 3. The error for SSD was up to two times smaller than for the SOBI approach. The histograms in Fig. 3 show also that in case of SOBI decomposition the errors were quite widely distributed and often exceeded 0.3. On the contrary, the errors obtained with SSD clustered around very small values having a very shallow right tail of the distribution. Overall SSD provided a satisfactory recovery of the source-patterns (error<0.1). The lower part of Fig. 3 shows also averaged errors for different SNRs. With very small SNR, i.e., at 0.01, the error in both decompositions became quite high and similar.

Real data

The SSD algorithm was also applied to the real EEG data recorded at rest for the extraction of alpha oscillations in the 8–13 Hz frequency band. SSD commonly resulted in clear patterns, corresponding to radial and tangential sources, located over sensorimotor and occipito-parietal areas (Fig. 4). Note that for the centrally-located sources the spectra have two characteristic peaks corresponding to the main frequency and its harmonic at twice higher frequency—a hallmark of the sensorimotor mu oscillations.

SOBI also resulted in patterns corresponding to radial and tangential dipoles. In some cases patterns obtained with ICA corresponded to those obtained with SSD. However when choosing components with the

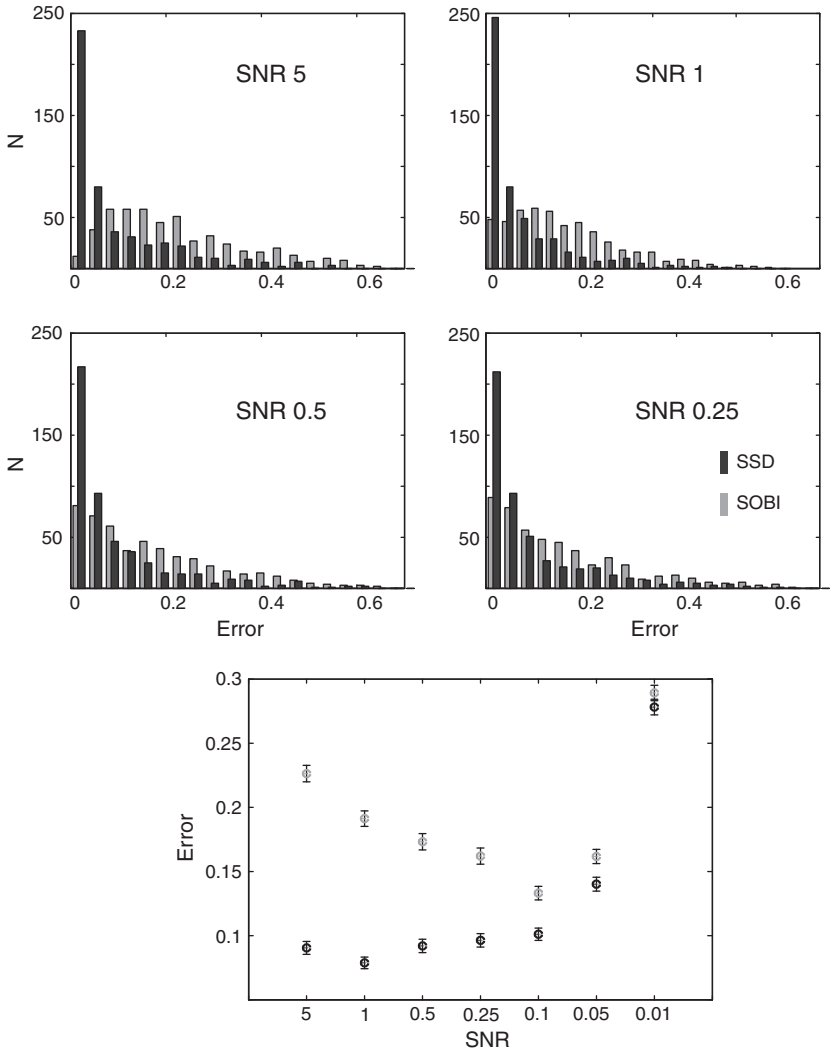

Fig. 3. The errors in recovering original patterns with SSD and SOBI algorithms for different SNRs. The upper four panels show distributions of errors for the different SNRs. The lower scatter-plot shows averaged errors for SNR from 5 to 0.01. Error bars are standard error of the mean.

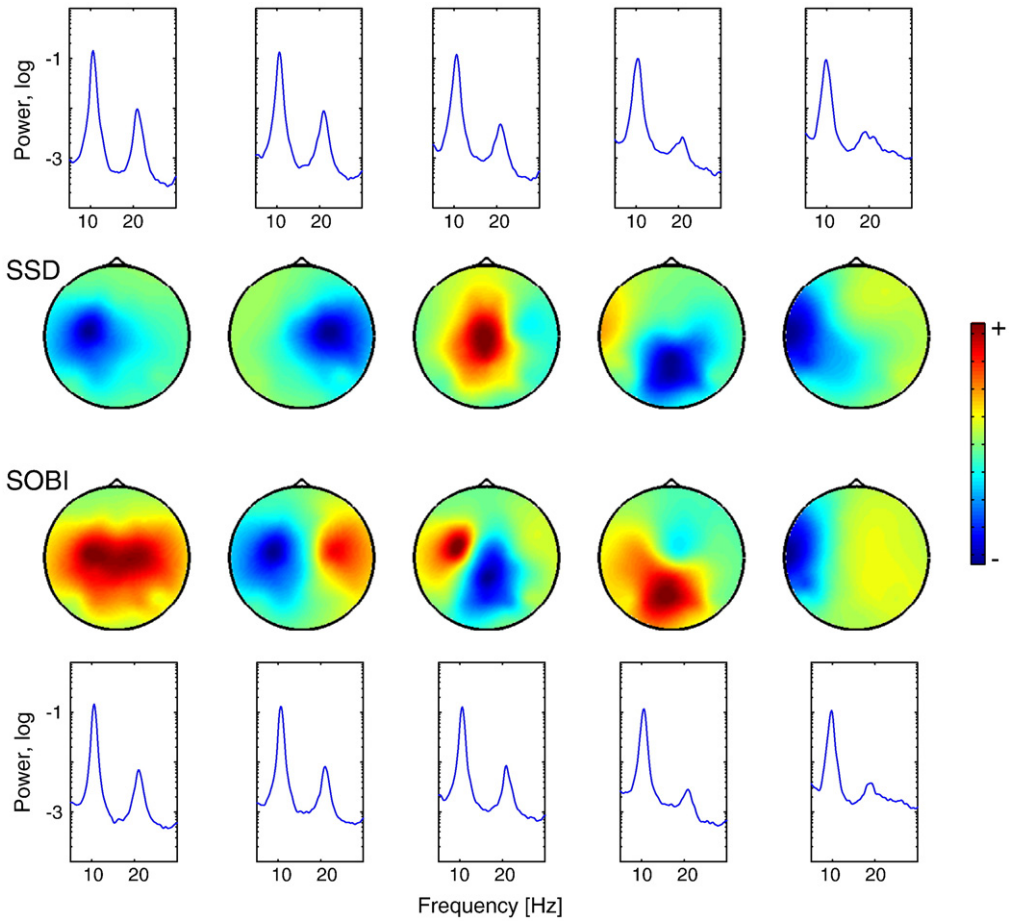

Fig. 4. Patterns and spectra of alpha oscillations extracted with SSD and SOBI algorithms from a real EEG recording for one typical subject. The color-scale is in arbitrary units. The components were sorted with respect to the spectral ratio defined in Eq. (24) (leftmost patterns correspond to the largest ratio).

strongest spectral ratio in the alpha frequency range (Eq. (24)) and comparing them to the patterns obtained with SSD, there often was a strong mismatch between the patterns. In order to quantify the similarity between the patterns obtained with SSD and SOBI we used an error estimate (Eq. (23)) for ten patterns with the strongest alpha power. In the present comparison the error does not indicate deviations from the true patterns like in the case of simulations, but rather it shows how similar the patterns were. The average error across seven subjects was ~0.25. The histogram of these errors (Fig. 5) shows that sometimes patterns obtained with SSD and SOBI were quite similar, with errors being smaller than 0.1. However, there were also many instances where the topographies differed substantially corresponding to errors exceeding 0.5. We also calculated spectral ratios (Eq. (24)) for SSD and SOBI, where the numerator was a mean of the spectral power in 8–13 Hz frequency range and the denominator—the combined mean spectral power in 6–8 and 13–15 Hz frequency ranges. In agreement with the basic idea of SSD its spectral ratios were larger than those corresponding to ICA decomposition ($P<0.001$, paired t-test), being 5.36 ± 0.7 and 4.68 ± 0.55, respectively.

In addition Fig. 6 shows how SSD works for the extraction of oscillations in neighboring frequency ranges. Figs. 6A–C show components with the strongest SNR when SSD was performed with different band-pass ranges (only one component for demonstration purpose): 8–13, 8–10 and 10–12 Hz, with flanking frequencies set as 2-Hz bands to the left and right from the cut-off frequencies of the band-pass range. Fig. 6D shows the spectra from the corresponding components. Note that 8–13 and 8–10 Hz frequency ranges include lower alpha—which to a certain extent is usually related to parietal areas. In agreement with this observation, patterns in Figs. 6A and B show activity over the posterior parts of the head. On the other hand, the component presented in Fig. 6C demonstrates that SSD was capable of recovering oscillations with a lateralized central distribution and spectral peak at about 11 Hz—which is typical for the sensorimotor oscillations.

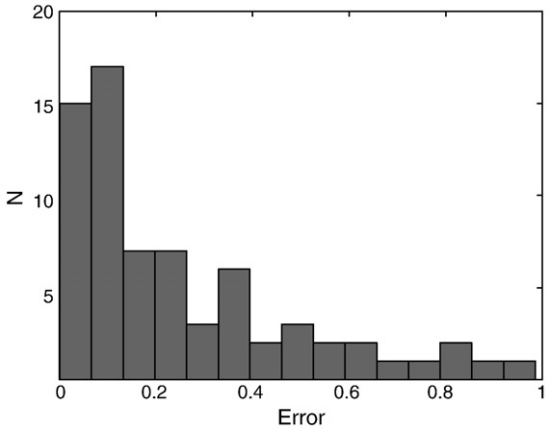

Fig. 5. Similarity between the patterns of alpha oscillations obtained with SSD and SOBI algorithms. The similarity is measured as an error index (smaller values indicate stronger similarity, Eq. (23)).

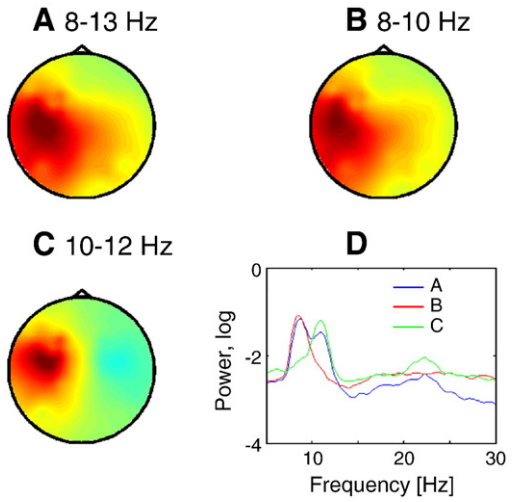

Fig. 6. Extraction of low and high frequency alpha oscillations with SSD. A, B and C: patterns corresponding to the largest eigenvalues for SSD performed on the basis of different band-pass filters in the range 8–13, 8–10 and 10–12 Hz, respectively. D. The spectra of the components corresponding to the patterns in A–C.

Computational time for SSD and SOBI

The computational time was estimated on a computer Pentium D 3.2 GHz, 2 GB RAM, using Matlab 7.1, Windows XP. An average time for performing SSD and SOBI algorithms on a simulated data ($n=150$, performed as described above) was $0.006 \pm 2e{-}05$ and 241 ± 8 s, respectively. The time estimation did not include filtering and calculation of the covariance matrices. The time required for the calculation of one covariance matrix was 0.099 ± 0.001 s and for one band-pass filtering (of 64-channel dataset) 0.58 ± 0.002 s.

Discussion

In this paper we introduced a novel approach for the extraction of oscillatory activity from EEG/MEG recordings. The simulations and real data analysis showed that SSD is an algorithm allowing fast and reliable extraction of neuronal oscillations.

Generalized eigenvalue decomposition has been previously used in EEG research in another context. i.e., for the extraction of spatial patterns from different experimental conditions recorded at separate time intervals (Blankertz et al., 2008; Koles, 1991, Common Spatial Patterns technique). To extract narrow-band activity, Sameni et al. (2010) suggested to use a ratio between the power in the given frequency band and power in a full Nyquist frequency range. However, it is not clear what this maximization means in terms of optimizing signal extraction in a given frequency band. In the present study we used a generalized eigenvalue decomposition in order to enhance the signal in a specific frequency band of the spectrum while simultaneously minimizing the noise power in the neighboring "surrounding" frequency bins. This procedure proved to be directly related to the optimization of SNR and the extraction of the neuronal sources.

Predefined frequency content of oscillatory activity

The SSD algorithm is based on the idea of using frequency bands which might be known *a priori* as being important/relevant for the neuronal processing in the brain. Indeed, a vast majority of previous EEG/MEG research showed that different cognitive, perceptual and motor processes require neuronal operations manifested at the specific frequency ranges (Buzsáki and Draguhn, 2004; Varela et al., 2001). Such specification of the frequency bands in SSD might allow an extraction of functionally relevant oscillatory components. Depending on the studied oscillations one should either widen or narrow filters in order to obtain spectral profile typical for the studied oscillatory patterns. Although recorded EEG and MEG signals often have peaks in the alpha and beta frequency ranges they are not necessarily pronounced, especially in the frontal and central areas. There, these peaks often do not stand clearly above the *1/f* part of the spectra. Applying Laplacian transformation, for instance, allows recovering shallow peaks which otherwise are hidden in the background noise. The idea of SSD is to enhance SNR by taking into account spatial structure of the noise. If the flanking frequency bins would contain other oscillations then SSD would in addition work through contrasting oscillations at different frequency bins. In this case SSD would find components with small power in one frequency bin and large power in another. In this case the separation from *1/f* part of noise will not be perfect, yet SSD would still allow extraction of the oscillations within the band-pass range. This might be particularly useful for contrasting low and high frequency alpha oscillations (Fig. 6). For instance, if one is interested in the differentiation of the low (8–10 Hz) and high frequency (10–12 Hz) alpha oscillations, then the "signal" filters might be centered at exactly these narrow frequency ranges, while surrounding "noise" frequency ranges could be fixed at 6–8/10–12 and 8–10/12–14 for slower and faster alpha oscillations, respectively.

As an alternative to predefined frequencies of interest, one can first study spectra of EEG/MEG signals in the sensor space, identify pronounced peaks and then define the frequency ranges for the signals of interest.

In case of the evoked gamma (Rodriguez et al., 1999) one can first estimate the frequency content from the averaged data and then use it for defining the filters to be applied to the raw data processing with SSD. Similarly, when studying ERD/ERS phenomena (Pfurtscheller and Lopes da Silva, 1999) one can first observe the frequency range with the most prominent changes in the amplitude dynamics of oscillations in the averaged data and then tailor the filters for SSD accordingly. Such estimation of the spectral content through the initial averaging would allow defining frequency bands even in the case when spectral peaks are not sufficiently visible in the raw data. Alternatively, if no peaks are visible one can perform SSD for different center frequencies f (Supplementary material).

An important area of application for SSD might be the extraction of oscillatory signals related to steady state evoked responses, which produce clear peaks in the spectrum at the frequency of stimulation (Regan, 1989). This would be relevant for the extraction of evoked potentials induced by rapid repetitive presentation of visual, auditory or somatosensory stimuli.

SSD extracts time courses of the neuronal sources (not necessarily single dipoles) as well as their topographies, which can be used for the localization of such sources within the brain using inverse modeling techniques.

SSD in comparison to other frequently used techniques for the analysis of oscillatory activity

Very often neuronal oscillations are analyzed on the basis of the signals directly obtained from EEG/MEG sensors. The major drawback of this simple approach is that the recorded activity represents a massive superposition of the signals from multiple sources, thus not allowing studying activity from the specific cortical areas. Beamformer techniques (Van Veen et al., 1997; Vrba and Robinson, 2001) allow a refined extraction of neuronal signals from the specific cortical locations. However, for very accurate results, this approach requires detailed information about the anatomy of the brain obtained with MRI, which is not always available. Moreover, use of beamformers does not guarantee an extraction of oscillatory components with the strongest SNRs as in the case of SSD. Interestingly, in case of SSD spatial filters are based on optimizing ratios between the neighboring frequency bins,

which might be analogues to a certain extent to the optimization of the beamformer but in the spatial domain.

During the recent years ICA was used frequently for the analysis of EEG/MEG recordings (Hyvärinen et al., 2010; James and Hesse, 2005; Klemm et al., 2009; Makeig et al., 2004). We used one of the popular algorithms—SOBI (Joyce et al., 2004; Tang et al., 2005) and compared it with the performance of SSD. In our simulations SSD recovered the patterns of the original sources with an error about half of that of SOBI in a quite broad SNR range (down to 0.05). This range approximately corresponds to a situation in EEG/MEG recordings where one frequently observes peaks above the *1/f* part of spectra in the conventional theta, alpha, beta and gamma bands. For the very low SNRs ~0.01 both decompositions resulted in large and similar errors. But this massive amount of noise might be considered as too extreme where in any case it is unlikely to recover reliably multiple neuronal sources.

Contrary to the simulations, in case of real EEG there is no possibility to know what are the true neuronal sources. Our analysis showed that SSD and SOBI might lead to the recovery of similar and also different patterns. Although it is not possible to confirm which of them are more realistic, we would like to note that SSD in addition allowed the recovery of the alpha oscillations with more pronounced spectral peaks, indicating better SNR. Another big advantage of SSD is that its calculation requires only a few milliseconds contrary to tens of seconds or even minutes in case of ICA, thus being at least 10,000 times faster. As with other decomposition techniques SSD should be used for recordings lasting for a few minutes.

In summary, SSD is an approach, which allows a reliable and fast extraction of neuronal oscillations in a predefined frequency range. In addition, the obtained oscillatory components have a maximized SNR, which in turn warrants the robust extraction of clear oscillatory signals.

Supplementary materials related to this article can be found online at doi:10.1016/j.neuroimage.2011.01.057.

Acknowledgments

GC and VVN acknowledge partial support by the Bernstein Center for Computational Neuroscience, Berlin. We thank Dr. Benjamin Blankertz and Dr. Steven Lemm for the discussions.

Appendix A

In source PCA and Minimum Overlap Component Analysis (Marzetti et al., 2008) field patterns were decomposed assuming that L2 minimum norm estimates of the true sources are approximately orthogonal in source space. If G is the $k \times l$ lead field matrix mapping l sources (including direction) to k sensors, for the topography $\vec{a}_i$ the source $\vec{s}_i$ is estimated as:

$$\vec{s}_i = G^T\left(GG^T\right)^{-1}\vec{a}_i$$

and two estimated sources, $\vec{s}_i$ and $\vec{s}_j$, are orthogonal if:

$$0 = \vec{s}_i^T\vec{s}_j = a_i^T\left(GG^T\right)^{-1}GG^T\left(GG^T\right)^{-1}\vec{a}_j = a_i^T\left(GG^T\right)^{-1}\vec{a}_j$$

which is equivalent to the orthogonality in the whitened space provided that $C_n = GG^T$ which holds (up to an irrelevant global constant) if the noise is dominated by the background neuronal activity.

References

Bell, A.J., Sejnowski, T.J., 1995. An information maximisation approach to blind separation and blind deconvolution. Neural. Comput. 7, 1129–1159.
Belouchrani, A., Abed-Meraim, K., Cardoso, J.-F., Moulines, E., 1997. A blind source separation technique using second-order statistics. IEEE Trans. Signal Process. 5, 434–444.
Blankertz, B., Tomioka, R., Lemm, S., Kawanabe, M., Müller, K.R., 2008. Optimizing spatial filters for robust EEG single-trial analysis. IEEE Signal Process. Mag. 25, 41–56.
Buzsáki, G., Draguhn, A., 2004. Neuronal oscillations in cortical networks. Science 304, 1926–1929.
Delorme, A., Makeig, S., 2004. EEGLAB: an open source toolbox for analysis of single-trial EEG dynamics including independent component analysis. J. Neurosci. Methods 134, 9–21.
Evans, A.C., Kamber, M., Collins, D.L., MacDonald, D., 1994. An MRI-based probabilistic atlas of neuroanatomy. In: Shorvon, S., et al. (Ed.), Magnetic Resonance Scanning and Epilepsy. Plenum, New York, pp. 263–274.
Fukunaga, K., 1990. Introduction to statistical pattern recognition2nd edition. Academic Press, Boston.
Hyvärinen, A., Oja, E., 1997. A fast fixed-point algorithm for independent component analysis. Neural. Comput. 9, 1483–1492.
Hyvärinen, A., Karhunen, J., Oja, E., 2001. Independent Component Analysis. John Wiley & Sons, New York.
Hyvärinen, A., Ramkumar, P., Parkkonen, L., Hari, R., 2010. Independent component analysis of short-time Fourier transforms for spontaneous EEG/MEG analysis. Neuroimage 49, 257–271.
James, C.J., Hesse, C.W., 2005. Independent component analysis for biomedical signals. Physiol. Meas. 26, 15–39.
Joyce, C.A., Gorodnitsky, I.F., Kutas, M., 2004. Automatic removal of eye movement and blink artifacts from EEG data using blind component separation. Psychophysiology 41, 313–325.
Klemm, M., Haueisen, J., Ivanova, G., 2009. Independent component analysis: comparison of algorithms for the investigation of surface electrical brain activity. Med. Biol. Eng. Comput. 47, 413–423.
Koles, Z.J., 1991. The quantitative extraction and topographic mapping of the abnormal components in the clinical EEG. Electroencephalogr. Clin. Neurophysiol. 79, 440–447.
Makeig, S., Debener, S., Onton, J., Delorme, A., 2004. Mining event-related brain dynamics. Trends Cogn. Sci. 8, 204–210.
Marzetti, L., Del Gratta, C., Nolte, G., 2008. Understanding brain connectivity from EEG data by identifying systems composed of interacting sources. Neuroimage 42, 87–98.
Nolte, G., Dassios, G., 2005. Analytic expansion of the EEG lead field for realistic volume conductors. Phys. Med. Biol. 50, 3807–3823.
Pfurtscheller, G., Lopes da Silva, F.H., 1999. Event-related EEG/MEG synchronization and desynchronization: basic principles. Clin. Neurophysiol. 110, 1842–1857.
Regan, D., 1989. Human Brain Electrophysiology: Evoked Potentials and Evoked Magnetic Fields in Science and Medicine. Elsevier, New York.
Rodriguez, E., George, N., Lachaux, J.P., Martinerie, J., Renault, B., Varela, F.J., 1999. Perception's shadow: long-distance synchronization of human brain activity. Nature 397, 430–433.
Sameni, R., Jutten, C., Shamsollahi, M.B., 2010. A Deflation Procedure for Subspace Decomposition. IEEE Trans. Signal Process. 58, 2363–2374.
Steriade, M., 2001. Impact of network activities on neuronal properties in corticothalamic systems. J. Neurophysiol. 86, 1–39.
Tang, A.C., Liu, J.Y., Sutherland, M.T., 2005. Recovery of correlated neuronal sources from EEG: the good and bad ways of using SOBI. Neuroimage 28, 507–519.
Van Veen, B.D., van Drongelen, W., Yuchtman, M., Suzuki, A., 1997. Localization of brain electrical activity via linearly constrained minimum variance spatial filtering. IEEE Trans. Biomed. Eng. 44, 867–880.
Varela, F., Lachaux, J.P., Rodriguez, E., Martinerie, J., 2001. The brainweb: phase synchronization and large-scale integration. Nat. Rev. Neurosci. 2, 229–239.
Vrba, J., Robinson, S.E., 2001. Signal processing in magnetoencephalography. Methods 25, 249–271.
Ziehe, A., Nolte, G., Curio, G., Müller, K.-R., 2000. OFI: optimal filtering algorithms for source separation. In: Pajunen, P., Karhunen, J. (Eds.), Proc. of the 2nd Intern. Workshop on Independent Component Analysis and Blind Signal Separation. Helsinki University of Technology, Helsinki, pp. 127–132.
Ziehe, A., Laskov, P., Nolte, G., Müller, K.-R., 2004. A fast algorithm for joint diagonalization with non-orthogonal transformations and its application to blind source separation. J. Mach. Learn. Res. 5, 801–818.